

# SUPPLEMENTARY INFORMATION

## A mass-spring model unveils the morphogenesis of phototrophic *Diatoma* biofilms

K. Celler, I. Hödl, A. Simone, T. J. Battin, C. Picioreanu

### A. Supplementary Methods

### B. Supplementary Data

**Table S1:** Computational model parameters

**Table S2:** Spring constant sensitivity analysis

**Figure S1:** Simulations for sensitivity analysis of spring constants

**Video SV1:** Animation of the model simulation for *Diatoma* colony formation at river *ridge* conditions (corresponding to Figure 4a-d)

**Video SV2:** Animation of the model simulation for *Diatoma* colony formation at river *valley* conditions (corresponding to Figure 4e-h)

## A. SUPPLEMENTARY METHODS

In this section, more detail is provided for the model processes described within the *Methods* section of the main manuscript.

### S.1 Mass-spring *Diatoma* model

A *Diatoma* cell, effectively cylindrical in shape, has dimensions of approximately  $R = 5 \mu\text{m}$  radius by  $L = 50 \mu\text{m}$  length. A chain of cells consists of several roughly cylindrical *Diatoma* cells attached to one another with extracellular polymeric substance (EPS) in a zigzag formation with an angle of roughly  $120^\circ$  between adjacent cells. The *Diatoma* chain is modelled as an array of particles with mass, connected by three spring types, which build rigid cells, keep angles between cells and ensure the zigzag conformation of the chain (see Figure 2). Chain movement is determined by the motion of each individual particle of that particular chain.

### S.2 *Diatoma* chain movement

#### S.2.1 Equations of motion

*Diatoma* colony formation was modelled in a three-dimensional Cartesian coordinate system. The vertical component of the system is limited by the substratum position at  $z = 0$ , but there is no restriction on colony height development at  $z > 0$ .

#### S.2.2 Drag and lift forces

Movement of *Diatoma* chains is a function of water flow, with both the strength of the flow and its direction taken into account. Without water flow, the force of gravity would pull the filaments down to the substratum. The flowing water exerts drag and lift forces on the cells, which push the filaments to and from the substratum and keep them in motion. The drag force  $\mathbf{F}_D$  acts on each *Diatoma* cell in the same direction as the relative water velocity, while the lift force  $\mathbf{F}_L$  is perpendicular to the drag.

In general, the magnitude  $F_D$  of the drag force of water on an obstacle is given by  $F_D = 0.5 C_D \rho_w U^2 A$ , where  $C_D$  is the drag coefficient,  $\rho_w$  is the density of water ( $\text{kg/m}^3$ ),  $U$  is the

relative velocity of water with respect to obstacle (m/s) and  $A$  the cross-sectional area of obstacle ( $\text{m}^2$ ), in this case the projected area of the *Diatoma* cylinder<sup>1</sup>. The drag coefficient  $C_D$  is a function of the Reynolds number,  $Re_D = UD\rho_w/\eta_w$ , which is defined relative to the *Diatoma* cylindrical body diameter,  $D$ , and the relative velocity,  $U = u - v$  (where  $u$  and  $v$  are the velocity magnitudes of water and cylinder, respectively). *Diatoma* cells living near the river bed experience  $Re \ll 1$ , which indicates Stokes flow dominated by the viscous forces in the liquid.

An important model assumption was the simplified one-way fluid-structure interaction: while the *Diatoma* filaments are moved by the flow, the flow itself is not affected. A measured dynamic flow velocity profile  $\mathbf{u}(t)$  is therefore imposed on the filaments. Water velocity  $\mathbf{u}$  was measured in the river flumes where the *Diatoma* experiments were carried out at the WasserCluster Research Centre using Laser Doppler Anemometry (LDA). For a description of the technique and measurements obtained, see reference 2. Although measurements were made for the  $x$ -,  $y$ - and  $z$ -directions ( $u_x$  downstream,  $u_y$  sideways and  $u_z$  along the depth axis, respectively) analysis indicated that the depth-axis measurements were inaccurate. Therefore, only velocity values from the  $x$ - and  $y$ -directions ( $u_x$  and  $u_y$ ) were considered for the simulation. Polar charts of the velocity magnitude and orientation at the ridge (Figure 1A) and valley (Figure 1B) indicate that at the ridge the velocity has a greater magnitude and is directed along with the flow, whereas at the valley the flow is slower and multidirectional. At model initialization, data from water velocity measurements was read into velocity vectors  $\mathbf{u}$ , used during the simulation. Because only 50 data points were available per second, while for the filament movement simulation denser data points were needed, linear interpolation was used to determine approximate values at intermediate time points. The water velocity profile over height  $u_z(z)$  was assumed to be linear, with  $u_z(0) = 0$  at substratum and  $u_z(500 \mu\text{m}) = 100 \mu\text{m/s}$ . This assumption is supported by the fact that the measured thickness of the laminar sublayer was  $800 \mu\text{m}$  in the valley and  $400 \mu\text{m}$  at the ridge positions, which are larger values than the modelled *Diatoma* colony heights. The model colonies were thus contained within the approximately linear region of the laminar sublayer.

Each chain consisted of multiple *Diatoma* cells, each cell being approximated by a cylinder. At these conditions, the drag coefficient on a circular cylinder normal to the flow,  $C_{D,n}$ , is given by the Oseen-Lamb laminar theory<sup>1</sup> as  $C_{D,n} = 8\pi / [Re_D \ln(7.4/Re_D)]$ . Filament movement throughout the system results in additional complexity when computing the drag coefficient. First, since

water velocity is estimated to depend linearly on the height above the streambed, the drag coefficient is computed at different  $Re_D$  over the height of the system. Second, the drag force is applied to cylinders in all possible orientations moving at various velocities. The independence or cross-flow principle<sup>1</sup> states that at an angle of attack, the flow pattern and fluid-dynamic pressure forces of a body only correspond to the velocity component in the direction normal to the cylinder axis<sup>2</sup>. The drag and lift coefficients can therefore be adjusted for the direction considering  $C_D = C_{D,n} \sin^3(\alpha)$  and  $C_L = C_{D,n} \sin^2(\alpha) \cos(\alpha)$ , with angle  $\alpha$  defined as the angle of inclination in respect to the flow. Given *Diatoma* axis orientation vector  $\mathbf{d}$  and the relative velocity vector ( $\mathbf{U} = \mathbf{u} - \mathbf{v}$ ) of the middle of a *Diatoma* segment, the angle  $\alpha$  between the vectors is  $\alpha = \cos^{-1}[(\mathbf{d} \cdot \mathbf{U})/(dU)]$ . The total force exerted by water per cell is equally divided between the end particles of a cell. Therefore, the magnitude of the drag and lift forces per particle is:

$$F_D = 0.25 \rho_w U^2 A C_{D,n} \sin^3(\alpha) \quad (i)$$

$$F_L = 0.25 \rho_w U^2 A C_{D,n} \sin^2(\alpha) \cos(\alpha) \quad (ii)$$

Vectors  $\mathbf{F}_D$  and  $\mathbf{F}_L$  lie in the plane defined by the axis of the *Diatoma* cylinder and the velocity vector  $\mathbf{U}$ . The drag vector  $\mathbf{F}_D$  acts in the same direction as the relative velocity  $\mathbf{U}$ . The direction of the lift vector  $\mathbf{F}_L$  is perpendicular to the drag. For the vertex particles that join two *Diatoma* cells, contributions from drag and lift from both cells are added.

### S.2.3 Elastic forces

Elastic forces keep the particles together in the form of zigzagged chains. Three types of elastic forces acting in linear springs connecting particles were designed to (Figure 2C): 1) keep the cell body rigid by opposing cell elongation and compression ( $\mathbf{F}_{E1}$ ); 2) keep two adjacent cells under a certain angle by opposing bending ( $\mathbf{F}_{E2}$ ); and 3) keep the chain zigzags by impeding torsion ( $\mathbf{F}_{E3}$ ). A linear spring connects two particles  $i$  and  $j$  situated at positions  $\mathbf{x}_i$  and  $\mathbf{x}_j$ . The spring is defined by a vector  $\mathbf{l}_{ij} = \mathbf{x}_j - \mathbf{x}_i$  (with  $l_{ij}$  being the length of the spring), a rest-length (equilibrium length)  $l_0$  and stiffness  $K_E$ . According to Hooke's law, the force exerted by a linear spring on particle  $i$  is:

$$\mathbf{F}_E = -K_E \frac{\mathbf{l}_{ij}}{l_{ij}} (l_{ij} - l_0) \quad (iii)$$

and an opposite force  $-\mathbf{F}_E$  is applied on the particle  $j$  at the other end of the spring. The rest-length of the first-order springs ( $l_{0,1}$ ) is simply a *Diatoma* length  $L = 50 \mu\text{m}$ . The rest lengths of the second- ( $l_{0,2}$ ) and third-order ( $l_{0,3}$ ) springs are computed using trigonometry and considering the rest conformation of the chain of *Diatoma* cells. The spring constants  $K_{E,1}$ ,  $K_{E,2}$  and  $K_{E,3}$  were chosen in an empirical way by running the simulation with different assumed elasticity values and comparing the output with actual movies made at the WasserCluster Research Centre (Lunz am See, Austria).

Similarly to forces needed for the construction of one chain, sticking of different chains in several points was also implemented with elastic forces. Sticking forces  $\mathbf{F}_S$  were created between particles belonging to different chains when situated in close proximity, with a rest-length  $l_{0,S}$  and stiffness  $K_S$ .

#### **S.2.4 Collision forces**

Movement of *Diatoma* chains necessitated implementation of a collision detection and response algorithm to ensure that during movement each chain does not pass through itself, the other chains, or the ground. In collision detection between *Diatoma* cells, the chains are seen as a set of linear segments. The shortest distance between each two segments is computed and compared to a threshold value  $l_c = 2R$  (i.e., twice the *Diatoma* radius). If the distance is smaller than this value, collision response is triggered and a repulsive force  $\mathbf{F}_C$ , similar to the elastic forces  $\mathbf{F}_E$ , is applied to the two cells. This force should be applied at the point of closest distance between the segments, but since forces are applied to particles, the force is divided and applied to the end points of the *Diatoma*, distributed between the two particles according to its distance from each. Collision forces are calculated according to Hooke's law, with collision spring constant  $K_c$ . The length of the vector between the closest points is compared to the threshold value  $l_c$  and the difference taken as the spring deformation distance<sup>3</sup>. Similarly, a response force to cell collision with the substratum is triggered when the distance between a particle and substratum becomes less than  $l_c = 2R$ .

#### **S.2.5 Gravity and buoyancy forces**

The forces of gravity and buoyancy are combined and computed for each *Diatoma* cell as:

$$\mathbf{F}_g = (\rho_d - \rho_w)V_d \mathbf{g} \quad (iv)$$

where  $V_d$  is the volume of one cell with density  $\rho_d$ , with the assumption that it has a cylindrical shape with radius  $R$  and length  $L_l$ . Once computed for the whole cell, the force is equally distributed among the two end particles. The gravitational acceleration,  $\mathbf{g}$ , acts in the  $z$ -direction.

### S.3 *Diatoma* chain growth

At simulation initialization,  $f_0$  cells are attached to the substratum, each seeding a different chain. Each initial *Diatoma* cell is randomly given a specific age, between 0 and  $0.99 T_d$ . The division age  $T_d$  is the same for all cells during the whole simulation. Given that one *Diatoma* cell is located between the centres of two particles  $i$  and  $i+1$  within a chain, for cell division purposes the age of the *Diatoma* cell is taken as the age of particle  $i$ . The age of each particle increases during the simulation until division age is reached. At this point in time, cell division takes place by creating a new particle and resetting the age of the two particles to zero.

Marvan discussed theories of *Diatoma* division<sup>4</sup>. During division, perturbation of the prevalent *Diatoma* zigzag filament conformation may occur. However, experimental observations showed that the change in conformation either occurs rarely, or is a temporary phenomenon. Within the model, therefore, chain extension was always modelled by inserting a zigzag link to the chain. Not one, but two new particles must be added to the growing chain when the division age of one particle has been reached. This is necessary to preserve the prevalent zigzag configuration.

### S.4 Cell attachment

Attachment is the process in which cells stick to the substratum surface. Attachment involved adding a new chain consisting of three particles (ie. two *Diatoma* cells connected under the characteristic angle) to a randomly chosen position on the substratum base. Such an event was implemented to occur at the end of each growth step, based on attachment frequencies measured at the WasserCluster Research Centre. Rough counts in the riverbed valleys and ridges indicated an attachment frequency of  $r_{\text{attach,v}} = 3.74 \pm 1.32$  cells/day (valley) and  $r_{\text{attach,r}} = 1.74 \pm 0.55$  cells/day (ridge) for a measurement area of  $2.6 \text{ mm}^2$ . Maximum daily attachments (given an

attachment area of 1200  $\mu\text{m}$  by 1200  $\mu\text{m}$ ) were therefore approximated at two attachments in the valley, and one at the ridge.

## S.5 Cell sticking

Sticking between *Diatoma* chains is a natural occurrence which leads to the formation of striking colony architectures such as dreadlocks (in mostly unidirectional flow, such as at riverbed ridges) or dome-shaped structures (in multidirectional flow, such as in the riverbed valleys). It is unclear whether duration or force of contact between chains is important or other factors. It was suggested that silica spines and gelatinous threads increase effective body size and further encounter with other colonies<sup>5</sup>. They may also enhance the probability of entanglement, which was termed “morphological stickiness”. Flexible chains appear to have higher morphological stickiness, with stickiness defined as the ratio of adhesion rate to collision rate, and values ranging from 0 to 1<sup>6,7</sup>. Both of these rates are highly variable: collision rate is a function of particle concentration, size and the mechanism by which particles are brought into contact, (*ie.* flow, attachment or deposition), while adhesion depends mainly on the physicochemical properties of the particle surface. In the model, sticking was set to occur in 1 in 10,000 collisions (standard uniform distribution), with a maximum of three sticking events per movement time step. These values resulted in visually realistic colony architecture formation for the given system size and flow parameters.

## S.6 MODEL SOLUTION

The model attempts to represent formation of growing *Diatoma* filamentous colonies, put in a continuous motion by the liquid flow. Processes of movement, growth and attachment are looped through sequentially. In order to model the system processes efficiently and decrease simulation run-time, however, movement and growth were set to run at different time scales within unique time steps. The shortest time interval is that of movement,  $\Delta t_m = 1$  s. During this movement time interval, results (particle position, velocity, spring connections) are saved at each  $\Delta t_{m,s} = 0.01$  s. The noise created by the stochastic sticking events occurring within the movement interval was too low to affect significantly the error check. The ODE solver used to calculate the movement of cell chains proved to be very stable and accurate.

In comparison to movement, cell growth is a much slower process, therefore a growth time interval  $\Delta t_g = 3600$  s was set. The growth of each cell in the 3600 s interval is calculated by direct integration of the growth equation (thus no ODE solver is needed), while no flow-induced movement takes place (i.e., the structure is “frozen”). Detailed movement is only evaluated during a short period of 1 s during each growth interval. It was considered that due to the fast chain movement dynamics, this short interval provides enough characteristic information to be transferred at the larger time scale of growth. The model thus evaluates movement for the duration of 1 s, after which the growth time counter is increased by the growth step of 3600 s, and followed by as many successive movement-growth sequences as considered necessary. Sticking events occur within a movement time step  $\Delta t_m$  because they are a function of collisions during movement, whereas attachment events take place after every growth step  $\Delta t_g$ .

## REFERENCES

- 1 Sumer, M. & Fredsøe, J. *Hydrodynamics Around Cylindrical Structures*. (World Scientific Publishing Co. Pte. Ltd., 1997).
- 2 Hoerner, S. F. *Fluid-Dynamic Drag: Theoretical, Experimental and Statistical Information*. (Hoerner Fluid-Dynamics, 1965).
- 3 Ericson, C. *Real-time collision detection*. (Elsevier, 2005).
- 4 Marvan, P. To the Problem of Chain Formation in Benthic Living Fragilariaceae. *Arch. Hydrobiol./Suppl. 41, Algological Studies* **8**, 289-316 (1973).
- 5 Riebesell, U. Particle Aggregation during a Diatom Bloom .2. Biological Aspects. *Mar Ecol Prog Ser* **69**, 281-291, doi:Doi 10.3354/Meps069281 (1991).
- 6 Karp-Boss, L. & Jumars, P. A. Motion of diatom chains in steady shear flow. *Limnol Oceanogr* **43**, 1767-1773 (1998).
- 7 Engel, A. The role of transparent exopolymer particles (TEP) in the increase in apparent particle stickiness ( $\alpha$ ) during the decline of a diatom bloom. *J Plankton Res* **22**, 485-497, doi:DOI 10.1093/plankt/22.3.485 (2000).

## B. SUPPLEMENTARY DATA

**Table S1.** Computational model parameters.

Parameter Name	<i>Symbol</i>	Units	Value	Source	
<b><u>Movement</u></b>					
Time interval for saving data within a movement time step	$\Delta t_{m,s}$	s	0.010	Chosen	
Movement time step	$\Delta t_m$	s	1.000	Chosen	
<b><u>Hydrodynamic Parameters</u></b>					
Water velocity	$u_w$	m/s	varies	Measured <sup>1</sup>	
Water density	$\rho_w$	kg/m <sup>3</sup>	1000	Known	
<i>Diatoma</i> density	$\rho_d$	kg/m <sup>3</sup>	1100	Measured <sup>1</sup>	
<b><u>Diatoma Geometry</u></b>					
<i>Diatoma</i> radius	$R$	μm	5	Measured <sup>1</sup>	
<i>Diatoma</i> length	$L_l$	μm	50	Measured <sup>1</sup>	
<b><u>Mechanical Parameters</u></b>					
Spring Constants					
First order	$K_{E1}$	N/m	$0.5 \times 10^{-2}$	Chosen	
Second order	$K_{E2}$	N/m	$0.5 \times 10^{-2}$	Chosen	
Third order	$K_{E3}$	N/m	$0.5 \times 10^{-2}$	Chosen	
Particle-wall collision	$K_w$	N/m	$0.5 \times 10^{-3}$	Chosen	
Particle-particle collision	$K_c$	N/m	$0.5 \times 10^{-3}$	Chosen	
Sticking	$K_s$	N/m	$0.5 \times 10^{-3}$	Chosen	
Distance (Rest lengths)					
Every first particle	$L_1$	μm	50	Measured <sup>1</sup>	
Every second particle	$L_2$	μm	86.6	Calculated	
Every third particle	$L_3$	μm	132.3	Calculated	
Angle between <i>Diatoma</i>	$\theta$	degrees	120	Measured <sup>1</sup>	
Gravitational acceleration	$g$	m/s <sup>2</sup>	-9.8	Known	
<b><u>Growth</u></b>					
Initial number of filaments	$f_0$	-	varies (ie. 5)	Chosen	
Growth time step	$\Delta t_g$	s	3600 or 900	Chosen	
Division age	$T_d$	s	86400	Measured <sup>1</sup>	
<b><u>Attachment</u></b>					
Attachment area	x-direction	$L_x$	μm	1200	Chosen
	y-direction	$L_y$	μm	1200	Chosen
Frequency					
Valley	$r_{attach,v}$	cells/day/m <sup>2</sup>	$1.44 \times 10^6$	Measured <sup>1</sup>	
Ridge	$r_{attach,r}$	cells/day/m <sup>2</sup>	$6.69 \times 10^5$	Measured <sup>1</sup>	
<b><u>Sticking</u></b>					
Rest-length for sticking spring	$L_S$	μm	50	Chosen	
Sticking probability	$P_S$	-	1 in 10,000	Chosen	

<sup>1</sup> Measurements made by Iris Hödl, WasserCluster Research Centre, Lunz am See, Austria.

**Table S2.** Spring constant sensitivity analysis.

Spring Constants (N/m)	Case 1	Case 2	Case 3
$K_{E1}$	0.5	$0.5 \times 10^{-2}$	$0.5 \times 10^{-4}$
$K_{E2}$	0.5	$0.5 \times 10^{-2}$	$0.5 \times 10^{-4}$
$K_{E3}$	0.5	$0.5 \times 10^{-2}$	$0.5 \times 10^{-4}$
$K_w$	$0.5 \times 10^{-1}$	$0.5 \times 10^{-3}$	$0.5 \times 10^{-5}$
$K_c$	$0.5 \times 10^{-1}$	$0.5 \times 10^{-3}$	$0.5 \times 10^{-5}$
$K_s$	$0.5 \times 10^{-1}$	$0.5 \times 10^{-3}$	$0.5 \times 10^{-5}$

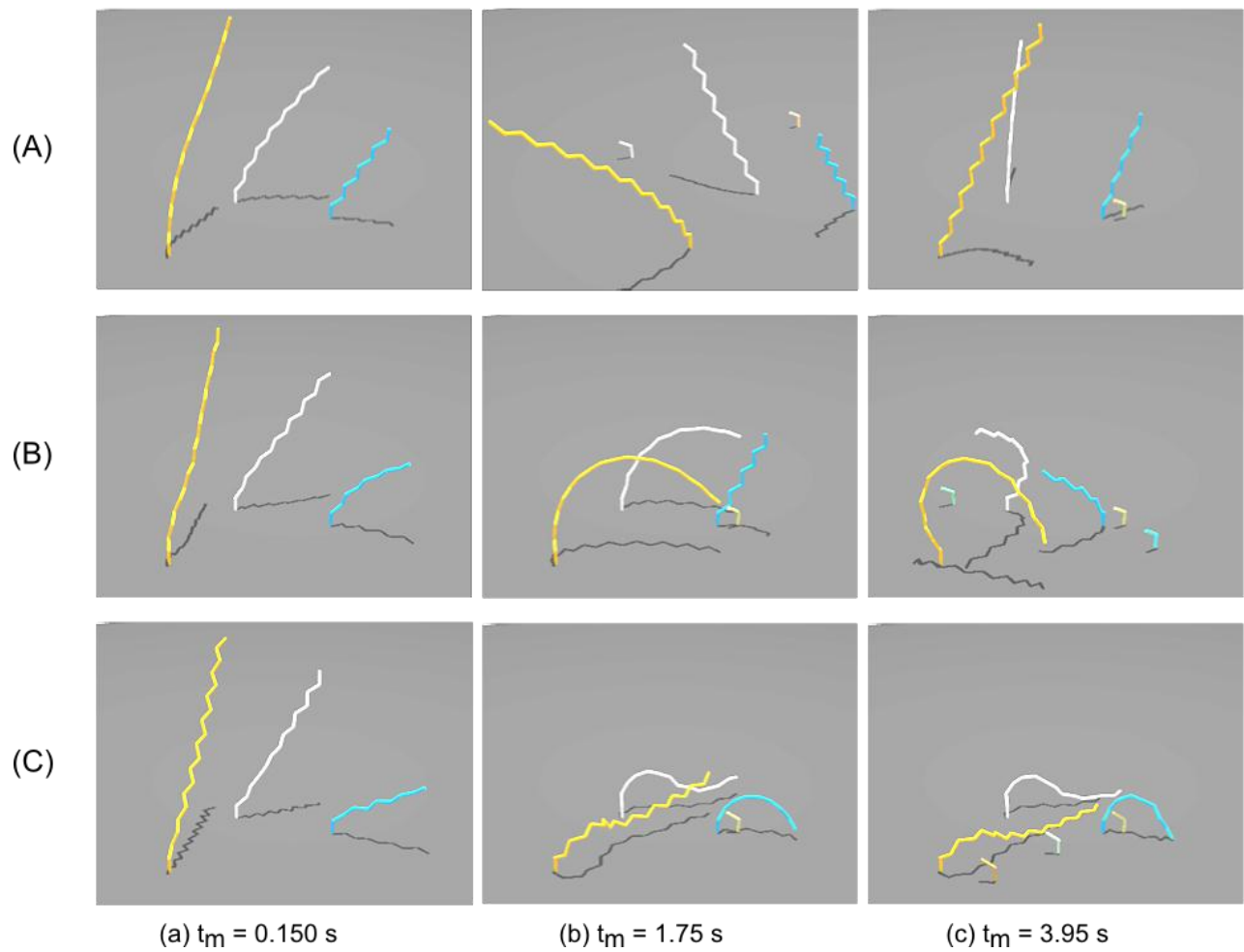


**Figure S1.** Simulations for sensitivity analysis of spring constants.

See Table S2 for the  $K$ -values for each case.

- (A) In Case 1, the spring constants are set to very stiff values. The water flow does little to move the filaments, and instead of bending over and forming bows, they remain upright.
- (B) Case 2 shows the preferred choice of spring constants such that "visually realistic" results are obtained. The filaments respond to the water flow, but still retain their required zigzag shape.
- (C) In Case 3, the spring constants are set to quite weak values. The filaments easily buckle under the flow, and the zigzag shape is deformed.